Time-of-Flight Flow Imaging of Two-Component Flow inside a Microfluidic Chip

Elad Harel, Christian Hilty, Katherine Koen, Erin E. McDonnell, and Alex Pines*

Materials Sciences Division, Lawrence Berkeley National Laboratory, and Department of Chemistry, University of California, Berkeley, California 94720, USA

(Received 6 August 2006; published 5 January 2007)

Here we report on using NMR imaging and spectroscopy in conjunction with time-of-flight tracking to noninvasively tag and monitor nuclear spins as they flow through the channels of a microfluidic chip. Any species with resolvable chemical-shift signatures can be separately monitored in a single experiment, irrespective of the optical properties of the fluids, thereby eliminating the need for foreign tracers. This is demonstrated on a chip with a mixing geometry in which two fluids converge from separate channels, and is generally applicable to any microfluidic device through which fluid flows within the nuclear spin-lattice relaxation time.

DOI: 10.1103/PhysRevLett.98.017601 PACS numbers: 76.60.Pc, 47.61.Ne, 82.56.−b

Microfluidic technology holds great potential for advancing research in a wide range of areas, for example, screening of ligand binding for drug development [1], as well as for performing fundamental studies of chemical, physical, and biological processes [2]. Naturally, fluid flow inside microfluidic chips plays a key role in their functioning and must be well understood to enable better device design for specific applications [3]. In this respect, finding methods to characterize the properties of the microfluidic device noninvasively and optimize the vast number of possible configurations and designs that govern efficiency and usability is critical.

Here we report on using NMR imaging and spectroscopy to investigate multiphasic fluid flow inside a microfluidic chip with a simple mixing geometry. To date, the most common method for monitoring mixing has been based on optical detection, which typically requires the use of a fluorescent dye or other foreign tracer [4]. However, optical detection suffers from a few serious drawbacks. For example, it is completely precluded in samples or sample environments that are opaque, confining it to chips fabricated from optically transparent materials. And while optical detection can provide chemical specificity, it can do so only in cases where the substance contains a chromophore, or where a molecular sensor has been designed to detect a specific substance [5]. Also, in some cases, addition of fluorescent dyes in a microfluidic system can alter the flow properties of the system through nonspecific interactions with the walls of the microchannels [6]. On the other hand, sensitivity is an inherent problem for absorption optical detection resulting from the short optical path length through microchannels [7].

Magnetic resonance (MR) is capable of bypassing some of those limitations. As an analytical technique NMR has achieved a significant impact across nearly all disciplines of science from structural biology [8] and drug discovery [9] to materials chemistry [10], to name just a few. Together with magnetic resonance imaging (MRI), it is a chemically sensitive method, suitable for microfluidic chip analysis provided that spin active nuclei such as hydrogen are present. Unfortunately, sensitivity has been a serious limitation to the more widespread use of magnetic resonance methods because the filling factor of the analyte in a microfluidic channel is very small due to the necessarily large coil that surrounds the chip. For purely spectroscopic applications, several groups have combated this limitation by fabricating surface coils directly onto the chip itself to increase sensitivity [11]. However, in addition to requiring a major effort in the way of chip fabrication which is not compatible with many of the more sophisticated chip designs already in place, such an approach enables acquisition of an NMR spectrum from only a single point on the device. Remote detection NMR provides a solution to both of these problems by physically separating the encoding and detection steps of conventional MR experiments so as to individually optimize each [12]. It is especially well suited for studies of flow as it naturally correlates spectroscopic or imaging information about the fluid or fluid environment with the time of flight (TOF) of the encoded nuclear spins from any location inside the sample to the detection region [13].

Previously, we have demonstrated the ability of the remote methodology to examine the flow of hyperpolarized ^{129}Xe gas inside a porous Bentheimer rock [13] and a single-channel microfluidic device [14]. More recently, we used the large chemical-shift sensitivity of ^{129}Xe to its local environment to characterize its flow and dispersion through a sample of silica aerogel by encoding for the chemical shift of xenon in different pore environments [15].

For molecules, in particular, liquids, each chemical species present shows a unique chemical-shift signature as it passes through the detector. This offers several advantages: first, it allows the flow from each species, regardless of the number, to be differentiated and thus imaged in a single remote experiment as long as resonances from different fluids are sufficiently resolvable and provided that each fluid reaches the detection coil on the order of T_1 after

encoding. For conventional, direct NMR detection, any magnetic field inhomogeneity across the entire microfluidic chip will lead to poor discrimination between the various nuclei, or the fluid channels may be too close in space for effective spatial selection. The advantage of the present method lies in the fact that because the fluids retain their chemical composition throughout travel to the detection region their NMR signature is preserved. Therefore, each species' fluid flow can be monitored separately by selecting out the appropriate peak or peaks in the spectra obtained in the detection coil. This concept is illustrated in Fig. 1 on a *T*-mixer chip with two inlets. The basic remote detection pulse scheme consisting of an encoding sequence, storage pulse, and stroboscopic detection is illustrated in Figs. 1(a)–1(c). The width of each travel curve [Fig. 1(d)] is a measure of the axial dispersion of the fluid flow, while the signal minimum is the most abundant TOF for travel from the encoding to detection region. More precise information is gained if a magnetic resonance imaging technique is applied during encoding, such as a gradient for phase encoding. Similarly, it is possible to encode chemical shifts, in which case a reconstructed interferogram is formed for each detection pulse [Fig. 1(e)].

We demonstrate the potential of this approach by studying mixing in a simple microfluidic chip. The chip contains two channels, each with a width of 200 μm and a depth of 100 μm, which converge at a T junction into one larger 400 μm wide channel. Pure ethyl alcohol flows through one of the channels and distilled water through the other.

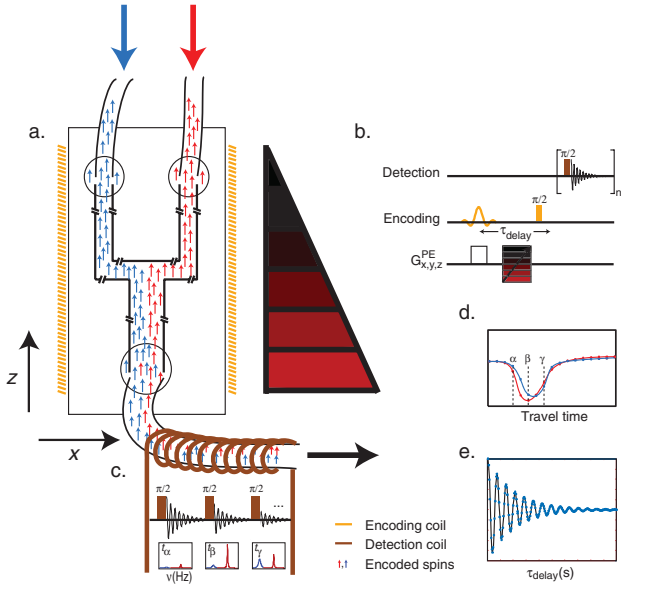

FIG. 1 (color). Schematic of a remote detection TOF imaging experiment applied to a microfluidic chip. (a) Fluids with different chemical-shift signatures (red and blue arrows) flow through each inlet channel before converging into the outlet channel. (b) Basic remote detection pulse sequence. See Refs. [12–16] for a more detailed description of remote detection NMR pulse sequences.

The encoding coil is a commercial imaging coil (Varian, Palo Alto, California) large enough to encompass the entire microfluidic chip. For detection, a small solenoid coil with a diameter of 500 μm was wound to allow a thin capillary (150 μm inner diameter) to pass through. Based on previous measurements, this coil is about 2 orders of magnitude more sensitive than the encoding coil for comparable volumes [16]. All experiments were performed on a Unity Inova NMR spectrometer (Varian Inc., Palo Alto, CA) at a magnetic field of 7.05 T, corresponding to a ^{1}H frequency of 300 MHz. Figure 2 shows a 2D representation of a remote spectral vs TOF dimension acquired by applying an incremented evolution time between the excitation and storage pulse and Fourier transforming the resultant indirect interferogram. The flow through each channel was adjusted so as to demonstrate that *a priori* knowledge of the origin of each fluid combined with such 2D spectral TOF data can give useful information about dispersion of each fluid's flow through the device even when full imaging is not possible due to experimental or measurement time constraints. In the resulting spectrum, the resonances stemming from the channel carrying ethyl alcohol are present at early times ($t_{travel} < 500$ ms), while the single peak from the channel carrying water arrives at a later time ($t_{travel} < 750$ ms). Notably, any natural magnetic field gradient across the chip will manifest itself in a change in the apparent chemical shift. In this regard, separating the chemical shift in the detection coil offers an advantage since such undesirable gradients in the encoding region do not affect the detected spectra.

Figure 2(b) shows the results of an experiment where spins were inverted in 2 mm slices parallel to the direction of flow. Signal at early times arises from spins encoded near the outlet of the chip, while later times correspond to the inlet region. Such remote inversion recovery experiments are a convenient and rapid method (<1 min) to measure dispersion along the channels. The dispersion as measured by remote detection is in fact a convolution of contributions from the flow inside the sample itself and from travel of the fluid from the sample to the detection coil. Considerable dispersion may arise during the travel time of the fluid as it travels from the outlet to the detection coil. However, it is still possible to compare the dispersion from two separate regions inside the chip because each must traverse the same path from the outlet to the detection coil.

Imaging was performed in a point-by-point fashion by phase encoding in reciprocal (k) space. Such indirect phase modulation is necessary in remote detection since the readout dimension, here replaced by a storage pulse, is not present as in conventional imaging or spectroscopy. The longer experiment time that arises due to this scheme is, however, compensated for by the additional time-of-flight information that is obtained. Figure 3 shows the results of a remote 2D time-resolved, flow imaging experiment in which each fluid is selected according to its spectra in the detection spectra [Fig. 3(b)]. This three-dimensional

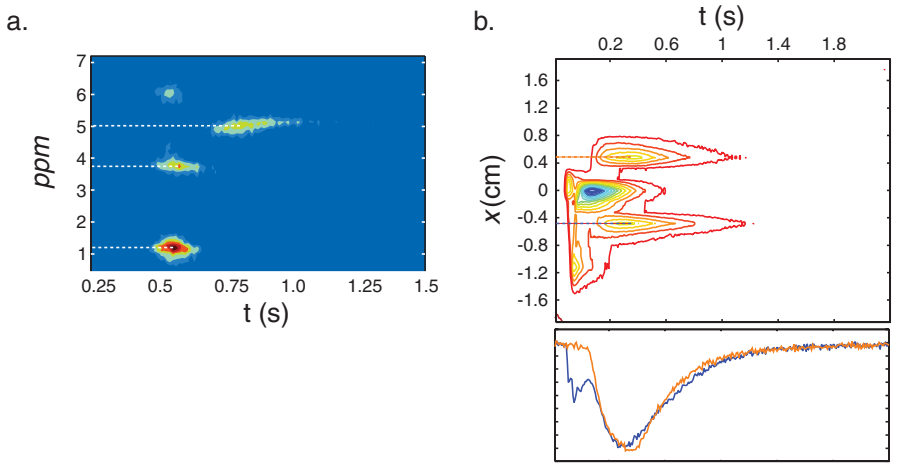

FIG. 2 (color). Frequency and spatial versus TOF dimension. (a) Remotely reconstructed spectrum of a 2.5 mm slice encoded across the chip, acquired by incrementing τ_{delay} and Fourier transforming the resulting interferogram. The flow rate of each fluid was adjusted to separate the resonances along the TOF dimension. (b) 2 mm slices along x were chosen by a combination of x gradient and rf pulse to give a π rotation of the magnetization. Blue (ethyl alcohol) and orange (water) curves in the lower panel represent cross sections taken at the position indicated by the dashed lines.

experiment contains dispersion data for any voxel inside the chip, allowing the two fluids' times-of-flight to be easily compared [Fig. 3(c)]. Because the acquisition for each detected spectrum is limited by the flow rates of encoded spins, a high time resolution necessarily implies poor spectral resolution in the detection coil as the residence time of the spins is rather short, on the order of 10 ms in this set of experiments. This time resolution, on the other hand, is sufficient to capture the relevant dynamics as shown in the higher-resolution image in the region following the T junction, which clearly shows that the two fluids do not mix while traversing the single-channel part of the microfluidic chip (Fig. 4). At the low Reynolds numbers of ethyl alcohol and water at the flow rates used here, this is not surprising for the current mixer geometry [17]. This experiment, however, highlights the potential of the presented remote detection methodology to evaluate the performance characteristics of any mixing geometry.

Using remotely detected time-of-flight NMR with chemical-shift selection, we have demonstrated a powerful

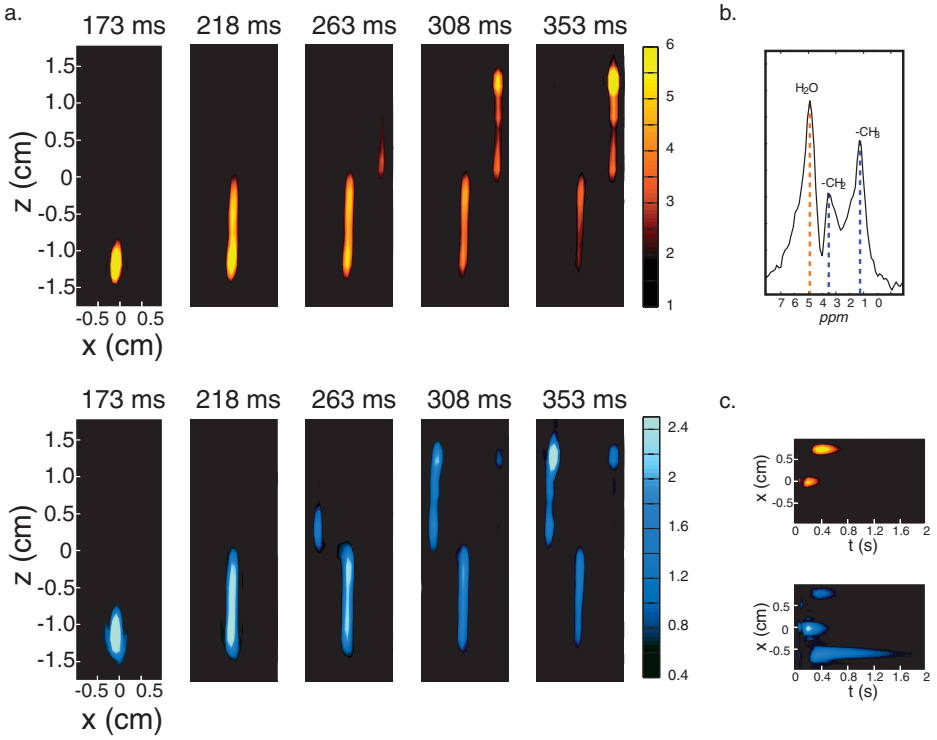

FIG. 3 (color). Time-resolved remotely detected images of spectrally resolvable fluid components. (a) Two-dimensional, phase-encoded remotely reconstructed partial images of water (red, top panels) and ethyl alcohol (blue, bottom panels) as they flow through the microfluidic T mixer. (b) Spectrum from the detection coil. Peaks that were chosen for the reconstruction of the images in (a) are marked with dashed lines of the corresponding color. Broadening of the peaks is due to a short residence time inside the detection coil. (c) Position in x versus time of flight obtained by projecting the three-dimensional data set along z.

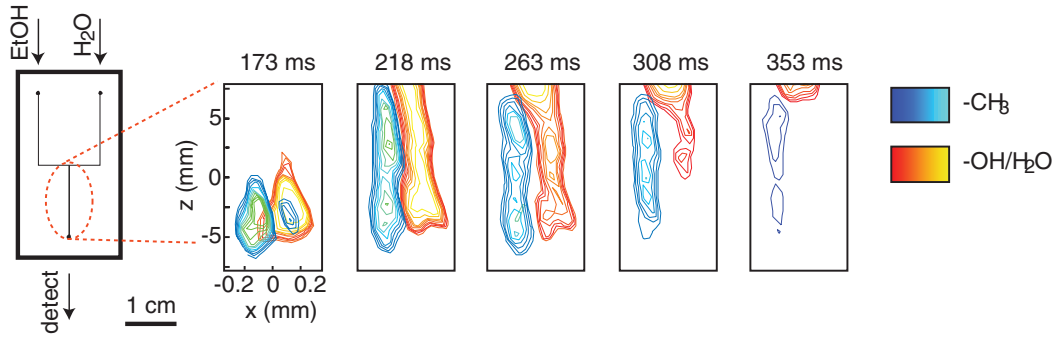

FIG. 4 (color). High-resolution time-resolved images of mixing inside the microfluidic chip. Contour plots of ethyl alcohol and water inside the outlet channel of the microfluidic chip. Resolution along x is 75 and 2.5 mm along z. The flow conditions were identical to those obtained for Fig. 3.

method for detecting fluid flow of multiple species inside a microfluidic chip, noninvasively. This offers significant advantages over optics-based methods as it does not require tracers or markers to be introduced into the fluid stream, and it allows the use of opaque materials for chip fabrication. As a means of detection, coupling magnetic resonance with microfluidics makes available the multitude of methods routinely used in high-resolution NMR spectroscopy and imaging. Future work will focus on imaging flow in chips with geometries designed to enhance mixing, for tracking chemical reactions, and monitoring protein dynamics.

We would like to thank T. Logan for help with microfabrication and J. Granwehr for helpful discussions. The microfluidic chip was fabricated in the Berkeley Microlab. E. H. is supported by the U.S. Department of Homeland Security under DOE Contract No. DE-AC05-00OR22750. This work is supported by the Director, Office of Science, Office of Basic Energy Sciences, and Materials Sciences Divisions of the U.S. Department of Energy under Contract No. DE-AC03-76SF0098.

*Corresponding author.
Electronic address: pines@cchem.berkeley.edu

[1] T. Chovan and A. Guttman, Trends Biotechnol. **20**, 116 (2002).
[2] J. W. Hong, V. Studer, G. Hang, W. F. Anderson, and S. R. Quake, Nat. Biotechnol. **22**, 435 (2004).
[3] H. A. Stone, A. D. Stroock, and A. Ajdari, Annu. Rev. Fluid Mech. **36**, 381 (2004).
[4] A. D. Stroock, S. K. Dertinger, A. Ajdari, I. Mezic, H. A. Stone, and G. M. Whitesides, Science **295**, 647 (2002).
[5] A. K. Singh, E. B. Cummings, and D. J. Throckmorton, Anal. Chem. **73**, 1057 (2001).
[6] D. Ross and L. E. Locascio, Anal. Chem. **75**, 1218 (2003).
[7] L. Zhu, C. S. Lee, and D. L. DeVoe, Lab Chip **6**, 115 (2006).
[8] K. Wuthrich, *NMR of Proteins and Nucleic Acids* (John Wiley & Sons, New York, 1986).
[9] P. J. Hajduk, R. P. Meadows, and S. W. Fesik, Q. Rev. Biophys. **32**, 211 (1999).
[10] P. T. Callaghan, *Principles of Nuclear Magnetic Resonance Microscopy* (Oxford University Press, Oxford, 1991).
[11] H. Wenink, F. Benito-Lopez, D. C. Hermes, W. Verboom, H. J. G. E. Gardeniers, D. N. Reinhoudt, and A. van den Berg, Lab Chip **5**, 280 (2005).
[12] A. J. Moule, M. M. Spence, S. I. Hans, J. A. Seeley, K. L. Pierce, S. Saxena, and A. Pines, Proc. Natl. Acad. Sci. U.S.A. **100**, 9122 (2003).
[13] J. Granwehr, E. Harel, S. Han, S. Garcia, A. Pines, P. N. Sen, and Y. Q. Song, Phys. Rev. Lett. **95**, 075503 (2005).
[14] C. Hilty, E. E. McDonnell, J. Granwehr, K. L. Pierce, S. I. Han, and A. Pines, Proc. Natl. Acad. Sci. U.S.A. **102**, 14 960 (2005).
[15] E. Harel, J. Granwehr, J. A. Seeley, and A. Pines, Nat. Mater. **5**, 321 (2006).
[16] E. E. McDonnell, S. I. Han, C. Hilty, K. Pierce, and A. Pines, Anal. Chem. **77**, 8109 (2005).
[17] An estimate for the Reynolds number is given by $R = \rho U h/\mu$, where ρ is the density, U is the mean velocity, h is the channel depth, and μ is the shear viscosity. For the data in Figs. 3 and 4 the flow rate was approximately 13 cm/s, giving a Reynolds number of about 15 for water and ethyl alcohol. At these low Reynolds numbers, flow is expected to be laminar, and the primary mixing mechanism is due to diffusion across streamlines. The Peclet number, which is defined as the ratio of convective to diffusive transport, is given by $\mathrm{Pe} = u_z h/D$, where D is the molecular diffusivity and u_z is the component of the velocity along the direction of flow. Under these experimental conditions it has a value greater than 10^2, indicating that convective transport is much faster than diffusive transport. The axial distance needed for complete mixing can be estimated by $\Delta z_m = \mathrm{Pe} \times h$, which gives a value of about 10 cm, significantly longer than the 1 cm region over which mixing is allowed to occur from the T junction to the outlet of the microfluidic chip.